

# The morphology of the stress-induced crystalline phase transition in poly(butylene terephthalate)

I. H. Hall\*† and E. A. Mahmoud‡

†Department of Pure and Applied Physics, UMIST, PO Box 88, Manchester M60 1QD, UK, and

‡Research Visitor from the Physics Department, Al-Azher University, Cairo, Egypt  
(Received 20 July 1987; revised 19 February 1988; accepted 7 March 1988)

The morphology of the stress-induced phase transition in poly(butylene terephthalate) is studied using small-angle X-ray scattering. The variation of scattered intensity with angle is recorded at several strains covering the range of the transition, and interpreted in terms of the linear paracrystalline model. The variation in the mean length of the crystalline and amorphous segments with strain is obtained, and also the variation in the widths of their distribution functions. It is shown that these changes cannot be accounted for solely by the transformation of  $\alpha$ -phase material into the  $\beta$ -phase, and that crystallization of the  $\beta$ -phase directly from amorphous material must also take place.

(Keywords: small-angle X-ray; poly(butylene terephthalate); stress-induced phase-transition; morphology)

## INTRODUCTION

It is well-established that when oriented poly(butylene terephthalate) (4GT) is subjected to stress the glycol residue changes from the *gauche-trans-gauche* conformation in the unstressed state to the all *trans* sequence under stress<sup>1,2</sup>. This has been related to the main features of the mechanical behaviour<sup>3</sup>, and has been shown to be a first-order cooperative phase transition<sup>4,5</sup>. However, Brereton *et al.*<sup>4</sup> point out that the physics of the nature of the cooperative interaction is very much an open question, requiring further investigation, and suggest three morphological possibilities which are consistent with their results.

The first is that boundaries between  $\alpha$  and  $\beta$  phases are generated in individual crystallites and move as stress increases. The second is that in the vicinity of very small crystallites local stress variations are of greater magnitude, causing these to transform first, and the third is that stress crystallizes small regions of the disordered material directly into the  $\beta$  form. Nothing has been done to distinguish between these possibilities.

Small-angle X-ray scattering (SAXS) is a very well-known technique for investigating the morphology of partially crystalline polymers. Whilst it is most frequently used in a qualitative manner the authors and their co-workers<sup>6</sup> have recently developed the technique to obtain a quantitative description of the morphology. They showed that the distribution of intensity of SAXS by oriented 4GT could be correctly predicted over the experimentally accessible range of scattering angles by a model in which fibrils along the orientation direction comprise alternating segments (amorphous and crystalline) of two different electron densities. These form linear paracrystals and the segment lengths are

distributed according to the Reinhold function<sup>7</sup>:

$$h(x) = \frac{x - \varepsilon}{(\gamma \langle Y \rangle)^2} \exp\left(\frac{-(x - \varepsilon)}{\gamma \langle Y \rangle}\right) \quad (1)$$

where

$$\varepsilon = \langle Y \rangle (1 - 2\gamma)$$

$x$  is the segment length,  $\langle Y \rangle$  the mean length and  $\gamma$  is a parameter controlling the skew and dispersion. The distributions of the lengths of the two types of segment were both described by the same equation, but with different parameters.

They describe a method which they have developed to determine the values of these parameters by minimizing the disagreement between the observed and calculated distribution of scattered intensity. For the final model, this disagreement is no greater than would be expected when the probable experimental errors in the intensity measurement are taken into account.

In the present work, this method is used to determine the way the segment lengths of 4GT change with applied strain. Since the electron densities of the  $\alpha$  and  $\beta$  crystalline phases are similar, SAXS will not distinguish between them, and the transition from one crystalline phase to the other cannot be observed directly. However, wide-angle X-ray scattering has been used to determine the proportions of  $\alpha$  and  $\beta$  crystalline phases as a function of applied strain<sup>4</sup>.

The two sets of experimental data are combined to deduce the way segment lengths change during the  $\alpha$ - $\beta$  phase transition. The results strongly favour a combination of the first and third mechanisms described above.

\* To whom correspondence should be addressed

## EXPERIMENTAL

The 4GT polymer was used in the form of an oriented ribbon, approximately 2 mm wide and 20  $\mu\text{m}$  thick. This was the same material as the authors used in their previous investigation<sup>6</sup> and from the same batch that was used by Brereton *et al.*<sup>4</sup> Characterization details may be found in these references.

A specially constructed specimen holder comprised two pegs around which the tape could be wound. These were approximately 50 mm apart and their separation could be controlled by a micrometer screw. Approximately 60 layers (which gave the maximum intensity of scattering) of tape were wound onto these with a small, constant tension being applied during the winding and the entire unit was then annealed for 20 h at a temperature of 205°C, during which time the specimen length was maintained constant. To reduce the effect of changes which were irreversible with strain, this was then very slowly (i.e. over a period of a day or two) increased to about 20% and relaxed until the tape was just taut. A gauge length was marked using a fine pen, and this is the length to which all subsequent strains refer. The sequence of operations was then to increase the length by a small amount, measure the strain using a travelling microscope, record the SAXS distribution, measure the strain again to ensure that no slipping had occurred, and then repeat for the next strain. Each sequence took approximately 1 day.

Since data were collected at eight different strains, the maximum being 16.8%, the complete experiment took about 2 weeks, during all of which the specimen was under strain. In a slow experiment like this, it is important to establish that time-dependent effects do not contribute to the change between the  $\alpha$  and  $\beta$  phases. This was investigated by Brereton *et al.*<sup>4</sup> who showed that there was no appreciable time-dependence in the transition process. The test-piece is therefore in a stable state during the data collection at any one strain, and this state is unlikely to depend upon the previous strain history.

The scattering was recorded using  $\text{CuK}\alpha$  radiation from the 0.1 mm square focus of a Marconi-Avionics GX-20 rotating-anode X-ray generator, with a Rigaku-Denki goniometer and a linear position-sensitive detector (LPSD) manufactured by Marconi-Avionics. Monochromatization was achieved by nickel filtration and energy discrimination at the detector. The beam was collimated by pin-holes of 0.5, 0.2 and 0.3 mm at distances of 120, 435 and 450 mm, respectively, from the source. The specimen was as close as practical to the third pin-hole and the detector plane was 300 mm from the specimen. The justification for these settings is given in a previous paper<sup>6</sup>, where it is shown that they provide the minimum parasitic scatter and the maximum beam intensity at which resolution is limited by the detector, and is about 0.05°. The distribution of scattering was recorded from an angle of about 0.3° (the extent of the back-stop shadow) up to about 2.5° (the limit of the LPSD).

Counts were recorded for  $6 \times 10^4$  s with the specimen in position, and for this time multiplied by the specimen transmittance with the specimen removed. This gave the background scatter which was later subtracted. The transmittance was measured using a weakened main beam. The counting time was chosen to give a small enough standard deviation in the number of counts per channel after background subtraction, and to enable the

measurements at each strain to be completed in a 24 h cycle.

The 512 channels of the LPSD recorded the scattering between angles of  $\pm 2.5^\circ$ . The central channel was chosen as that which maximized the symmetry of the two halves of the pattern. The counts on channels equidistant either side of this centre were then added. The angular separation of adjacent channels was determined in a separate experiment, and so the scattered intensity was obtained as a function of scattering angle. These were finally corrected for the spread of scatter transverse to the orientation axis by multiplying by the value of the scattering vector,  $s$  ( $= 2\sin\theta/\lambda$  where  $\lambda$  is the wavelength of the radiation), and scaled so that the maximum intensity was unity. Further details of the experimental procedure, and the justification for its use may be found in reference 6.

## TREATMENT OF DATA

We have shown<sup>6</sup> that the X-ray scattering distribution at small angles from 4GT can be described by the linear paracrystalline model of Hosemann<sup>8</sup>, where the segment lengths of both high and low density phases are distributed according to the Reinhold function (equation (1)). According to Hosemann

$$\frac{2I(\pi s)^2}{\Delta\rho^2} = \text{Re} \left[ \frac{1-H}{1-H_y J_z} \left\{ N(1-J_z) + \frac{J_z(1-H_y)\{1-(H_y J_z)^N\}}{1-H_y J_z} \right\} \right] \quad (2)$$

where  $I$  is the intensity of scattering by one paracrystal relative to that of a single electron placed at its centre,  $\Delta\rho$  is the electron density difference between the phases,  $H_y$  and  $J_z$  are, respectively, the Fourier transforms of the normalized distribution functions of the segment lengths of the phases  $y$  and  $z$ , and  $N$  is the number of repeating units in the paracrystal. Since we are only able to measure relative intensities, we calculate  $I/N\Delta\rho^2$  (which we shall subsequently refer to as  $I$ ) and from equations (1) and (2) this is a function of the five variables  $\langle Y \rangle$ ,  $\langle Z \rangle$ , (the mean lengths of the two phases),  $\gamma_y$ ,  $\gamma_z$  and  $N$ .

In our previous investigation<sup>6</sup>, we showed that provided  $N$  was greater than about 20, the intensity distribution was insensitive to its value, and that for smaller values only the intensities at very small angles ( $< 0.4^\circ$ ) were affected. The stepping refinement procedure developed in this earlier work was therefore used with  $N$  set at 20 to find the combination of values of the above variables which, together with the factor used to scale calculated to observed intensities, minimized the sum of  $\chi^2$  ( $(I_{\text{calc}} - I_{\text{obs}})^2/\sigma^2$ , where  $\sigma$  is the standard deviation of  $I_{\text{obs}}$ ) over all data points. The value of  $\sigma$  was determined from the experimental number of counts at each data point, taking account of the statistical error in the number of background counts.

We also showed that the only region of the scattering curve where poor agreement was obtained between  $I_{\text{obs}}$  and  $I_{\text{calc}}$  was at angles below about 0.5°, and that the best fit was achieved by omitting data collected at angles below about 0.55° from the refinement procedure. We therefore carried out several refinements, using different lower angles in the range 0.5–0.6°, and selected that at the lowest angle which gave good overall agreement.

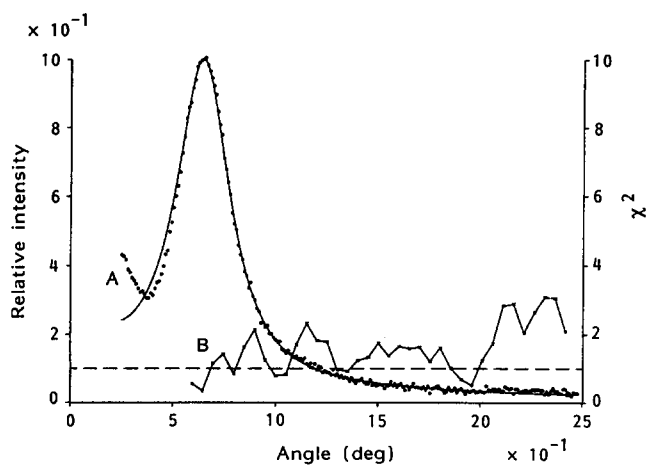


Figure 1 Observed intensities and those calculated for the model giving a best fit at 0.063 strain. The values of  $\chi^2$  are the means of 10 successive values. The continuous line is the calculated scatter. A, Experimental data; B,  $\chi^2$

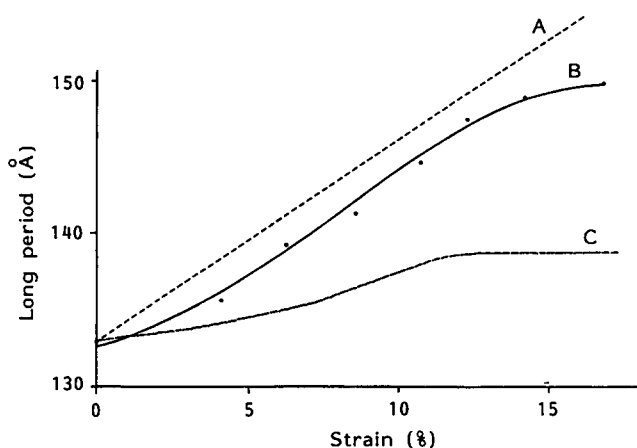


Figure 2 The variation of long period with strain. A, Expected change if the long period strain equals the applied strain; B, measured values; C, expected change if the increase in long period is due solely to the transformation of the  $\alpha$ -phase to  $\beta$ .

This procedure was followed at each of the strains, yielding the parameters describing the distribution of segment lengths of the high and low density phases as a function of strain. In Figure 1 the calculated and measured intensities, and  $\chi^2$  are shown for a strain of 0.063 as an example of the agreement which was achieved between the  $I_{\text{obs}}$  and  $I_{\text{calc}}$  distribution.

## RESULTS

The results are shown in Figures 2–4. A major uncertainty in the application of this technique is that the phases are not uniquely defined. Thus, it does not follow that the values which emerge for the parameters of phase Y from the refinement at one value of strain relate to the same phase as those for phase Y at any other strain. The values were assigned to phases on the assumption that discontinuous changes with strain in either segment length or  $\gamma$  were unlikely. As is clear from Figures 3 and 4, any other assignment than the one used would lead to such discontinuities. It is also not clear which of phases Y and Z refers to the high density (crystalline) phase, and which refers to the low density (amorphous) phase. To

make this assignment values of crystallite size obtained by Brereton *et al.*<sup>4</sup> were used. These were obtained from measurements of the width of the 104 and 106 reflections in the wide-angle pattern.

Our test-piece came from the same batch of material as that of Brereton *et al.*<sup>4</sup>; it was also subjected to the same annealing treatment and so crystallite sizes are likely to be similar. Brereton *et al.*<sup>4</sup> found that in the unstrained state the average thickness in the chain direction of the  $\alpha$  form was 62 Å and of the  $\beta$  form in the strained state was 75 Å. These values correspond more closely to the mean segment lengths of the Y phase at low and high strains than the Z phase, and so it is assumed that this is the crystalline phase.

The variation of  $\gamma$  with strain is shown in Figure 4 but the interpretation of this in terms of the changes in the distribution of segment lengths is not immediately apparent. As an example of this, the distributions of lengths of both phases are plotted in Figure 5. It is seen that although the mean lengths of the two phases are very different, this is due to the presence of long amorphous segments. The shorter segments of both distributions are of similar lengths.

A clearer idea of the changes taking place in the distribution is given in Figure 6. In Figure 6 the shortest length in the distribution and the length which is greater than that of 90% of the segments are plotted against strain.

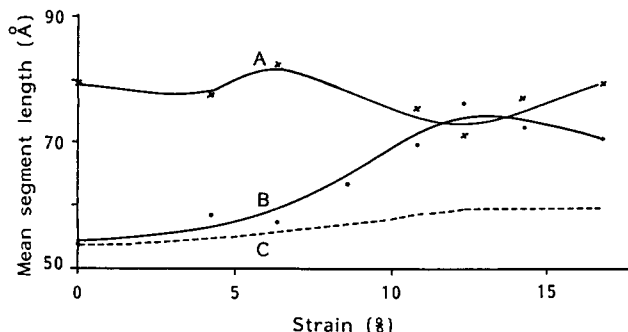


Figure 3 Variation of mean segment length with strain. A, phase Z (amorphous); B, phase Y (crystalline); C, the change in mean crystallite length expected if it is caused solely by the transformation of the  $\alpha$ -phase to  $\beta$

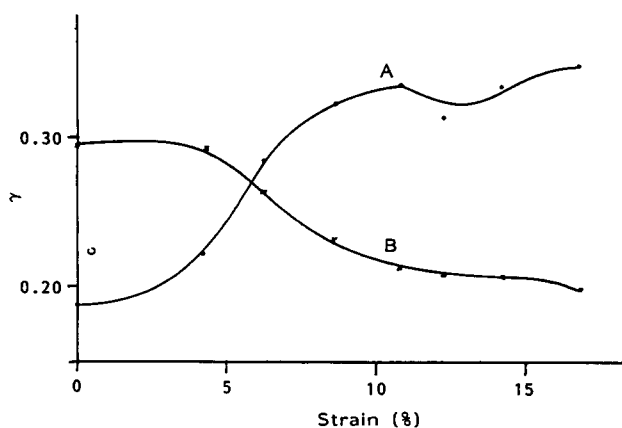


Figure 4 Variation of  $\gamma$  (dispersion of segment length) with strain. A, phase Y (crystalline); B, phase Z (amorphous)

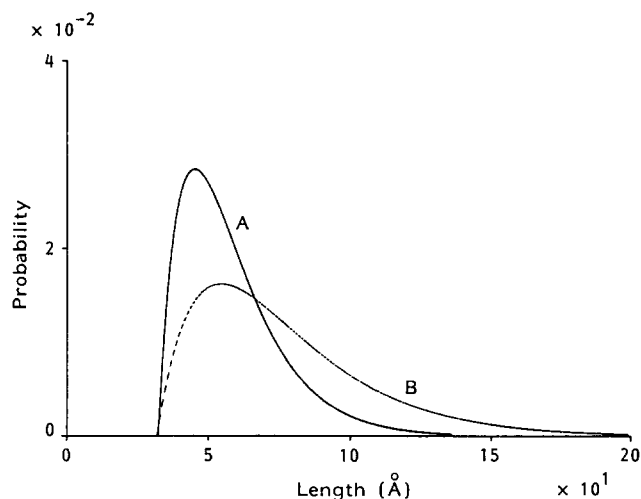


Figure 5 Probability distribution functions of lengths of crystalline and amorphous phases at strain of 0.042. A, Crystalline phase; B, amorphous phase

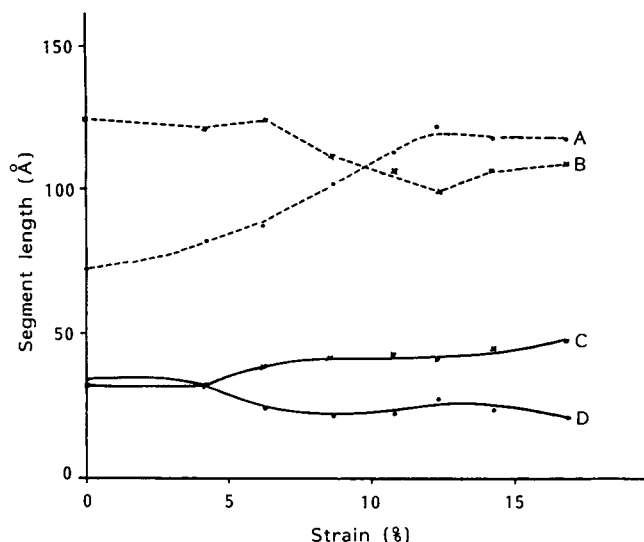


Figure 6 Variation of extreme segment lengths with strain. A, Crystalline and B, amorphous phase; length greater than that of 90% of the segments. C, Amorphous and D, crystalline phase; length of shortest segment

## DISCUSSION

At an intermediate strain there will be three phases present, the  $\alpha$  and  $\beta$  crystalline phases and the amorphous. However, the electron density difference between the two crystalline phases will be much less than that between either of them and the amorphous phase. Thus it is unlikely that the X-ray scattering will distinguish between  $\alpha$  and  $\beta$ ; it will only reveal the arrangement of crystalline and amorphous material. The results will be analysed on this assumption.

Brereton *et al.*<sup>4</sup> determined the change in the proportions of  $\alpha$  and  $\beta$  material with stress, by monitoring the intensities of wide-angle X-ray reflections characteristic of each phase. From their published data it is possible to calculate the proportion of crystalline material which is in the  $\alpha$ -phase at each of the strains used in this work. Since we have used material from the same batch, with the same annealing conditions, these proportions should be applicable to the present results (Table 1).

We shall first analyse the results on the hypothesis that boundaries between the  $\alpha$  and  $\beta$  phases are generated in individual crystallites, that these boundaries move as strain increases, and that this is the only change taking place. In this case, the increase in the long period with strain would be due entirely to the transformation of the existing  $\alpha$  material to  $\beta$  and can be calculated from the known unit cell dimensions<sup>9</sup>, the mean length of the crystalline segment in the unstrained state, and the information in Table 1. This calculated curve has been included in Figure 2 and shows that the measured increase is much greater than that calculated. Even if the crystalline phase has been wrongly assigned, and the longer of the two mean segment lengths is used in the calculation, the observed increase in the long period is still almost twice that predicted.

In the process of making this calculation, the mean segment length of the crystalline phase is obtained as a function of strain, and this curve is included in Figure 3. Whilst its sigmoidal shape corresponds with that observed, suggesting that transformation of  $\alpha$  to  $\beta$  material is taking place according to the proposed hypothesis, the length grows more than would be expected. At zero strain the mean crystalline segment length corresponds to 4.6  $\alpha$ -phase unit cells; at 14.2% strain it corresponds to 5.6  $\beta$ -phase cells.

If the proposed hypothesis were true, the lengths of segments of the amorphous phase would not change with strain. From Figures 3, 4 and 6 this is clearly not so. The mean length decreases by about 5 Å whilst the transformation takes place.

Whilst there is nothing in the results to indicate that transformation of crystalline material from the  $\alpha$  to the  $\beta$  phase is not taking place, all of the evidence discussed above clearly shows that this alone will not account for the observed results, and strongly suggests that, as strain is increased, amorphous material is being crystallized directly into the  $\beta$  phase. Let us assume that this crystallization occurs at the interfaces between the crystalline and amorphous segments.

If this was so, all amorphous segments would decrease in length by a similar amount, whatever their original length, and the crystalline ones would show a similar increase. Thus the dispersion of lengths would not change. Figure 6 shows that this is not so; the dispersion of the amorphous segment lengths decreases, whilst that of the crystalline increases. It is therefore necessary to postulate that crystallization is taking place elsewhere.

Examination of Figure 6 shows that the shortest amorphous segments increase in length from about 30 to about 40 Å and this suggests that crystallization occurs preferentially where neighbouring crystalline segments are separated by a very short amorphous one. They would then join together causing the shortest amorphous

Table 1 Proportion of crystalline material in the  $\alpha$  phase

Strain (%)	Fraction of $\alpha$
0.0	0.99
4.2	0.80
6.3	0.65
8.6	0.45
10.8	0.17
12.3	0.05
14.2	0.04

lengths to disappear from the population, and the proportion of very long crystallites to increase. *Figure 6* confirms that this occurs.

It also shows that the proportion of very long amorphous segments decreases. This would happen if the probability of nucleation of stress-crystallization increased with the length of the amorphous segment. Short  $\beta$ -phase crystallites would then be formed, dividing a very long amorphous segment into two short ones. *Figure 6* shows that such short crystallites are indeed formed.

Thus, to explain the results, it is necessary to postulate that as well as transformation of  $\alpha$ -phase crystallites into the  $\beta$ -phase, stress-crystallization of amorphous material directly into the  $\beta$ -phase occurs. This happens preferentially at two sites: in very short and in very long segments. For the former, the discontinuities might be expected to cause high local stresses favouring crystallizations. The latter would be expected on probability grounds. These correspond to the first and third of the possible mechanisms put forward by Brereton *et al.*<sup>4</sup> The crystallization of material not contained in the segmented stacks is unlikely to be important because the stack crystallinity (ratio of mean length of crystal segment to the long period) before strain and the bulk crystallinity by density are both about 40%, suggesting that either there is very little of this material, or that it has a very similar crystalline/amorphous ratio to that of the stacks.

The explanation might appear to be inconsistent with the observed reversibility of the phase change. Why should some  $\beta$ -phase crystallites revert to the  $\alpha$ -phase whilst others become amorphous? Very short crystals (these comprise only about two unit cells) might be expected to be unstable, in which case they would melt rather than transform on release of stress. The melting of a short segment incorporated into a long crystal is more difficult to explain. Although the small-angle scattering 'sees' this as an integral part of the crystal, there may well be defects invisible to SAXS which cause it to revert to the amorphous rather than the  $\alpha$ -phase.

If the amorphous and crystalline phases have been wrongly assigned in the interpretation of the scattering data, it is still necessary to postulate interchange between amorphous and crystalline material. In this case the 'amorphous' and 'crystalline' captions must be interchanged on the diagrams, when it will be seen that the lengths of the crystalline segments decrease, suggesting melting of some crystalline material. Such

melting is unlikely to occur with stress. Also the increase in the lengths of the amorphous segments is greater than the decrease in that of the crystallites and this is difficult to reconcile with the loss of order. Thus the present assignment seems unlikely to be wrong.

The Reinhold distribution of segment lengths has been assumed (equation (1)). The mean of  $\chi^2$  over all data points was about 1.4 and did not change significantly with strain. This value suggests that the discrepancies between the observed scattering and that calculated from the model were significant, and that the actual distribution might differ slightly from that assumed. However, we have shown<sup>6</sup> that other distribution functions, whilst not giving such a good fit to the observed scattering, lead to similar mean lengths and distribution widths. Thus a better distribution function would be unlikely to yield significantly different results.

Tashiro *et al.*<sup>5</sup> attempt to describe the mechanical properties of 4GT using a series model. They assume that the amorphous segments are unchanged during the transition from the  $\alpha$  to  $\beta$  phase which takes place at a constant stress, and that at other stresses elastic deformation of both types of segment takes place. Whilst our results do not invalidate the series concept, and *Figure 2* shows that most of the bulk strain is accounted for by changes in the length of the segmented stacks, the remainder of their assumptions represent an oversimplification. Most of the length change occurs because of the crystallization of amorphous material, and this must be included in any mechanical theory.

## REFERENCES

- 1 Yokouchi, M., Sakakibara, Y., Chatani, Y., Tadokoro, H., Tanaka, T. and Yoda, K. *Macromolecules* 1976, **9**, 266
- 2 Hall, I. H. and Pass, M. G. *Polymer* 1976, **17**, 807
- 3 Jakeways, R., Smith, T., Ward, I. M. and Wilding, M. A. *J. Polym. Sci., Polym. Lett. Edn.* 1976, **14**, 41
- 4 Brereton, M. G., Davies, G. R., Jakeways, R., Smith, T. and Ward, I. M. *Polymer* 1978, **19**, 17
- 5 Tashiro, K., Nakai, Y., Kobayashi, M. and Tadokoro, H. *Macromolecules* 1980, **13**, 137
- 6 Hall, I. H., Mahmoud, E. A., Carr, P. D. and Geng, Y. D. *Colloid Polym. Sci.* 1987, **265**, 383
- 7 Reinhold, C., Fischer, E. W. and Peterlin, A. *J. Appl. Phys.* 1964, **35**, 71
- 8 Hosemann, R., Bagchi, S. N. 'Direct Analysis of Diffraction by Matter', North Holland, Amsterdam, 1962
- 9 Hall, I. H. 'Structure of Crystalline Polymers', (Ed. I. H. Hall), Elsevier, London, 1984, p. 39